



THIN FIBER METAL LAMINATE: EXPERIMENTAL AND ANALYTICAL DETERMINATION OF STIFFNESS AND STRENGTH FOR VARIOUS FIBRE ORIENTATIONS

Murni Awi^a, Ahmad Sufian Abdullah^{a,b*}, Aslina Anjang Ab Rahman^c, Kamarul-Azhar Kamarudind^d

^a Centre for Mechanical Engineering Studies, Universiti Teknologi MARA, Cawangan Pulau Pinang, Permatang Pauh, Pulau Pinang, 13500, Malaysia

^b Advanced Mechanics Research Group, Centre for Mechanical Engineering Studies, Universiti Teknologi MARA, Cawangan Pulau Pinang, Permatang Pauh, Pulau Pinang, 13500, Malaysia.

^c School of Aerospace Engineering, Universiti Sains Malaysia, Nibong Tebal, Penang, 14300, Malaysia

^d Crashworthiness and Collisions Research Group (COLORED), Faculty of Mechanical and Manufacturing Engineering, Universiti Tun Hussein Onn Malaysia, Batu Pahat, 86400 Johor, Malaysia

ARTICLE INFO

ARTICLE HISTORY

Received: 10-01-2023

Revised: 05-03-2023

Accepted: 20-04-2023

Published: 30-06-2023

KEYWORDS

Fiber metal laminate (FML)

Glass fibre composite

Mechanical characteristic

Metal volume fraction (MVF)

method

ABSTRACT

This paper aims to determine the stiffness and strength of fibre metal laminate (FML) with various fibre orientations, as well as the efficiency of rule of mixture prediction on thin FML with various fibre orientations. FML and GFRP were fabricated from prepreg. All the specimens were prepared by adopting the ASTM D3039 testing standard and the thickness of GFRP and FML were 0.83 mm ~ 0.85 mm and 1.39 mm ~ 1.50 mm, respectively. The tensile tests were performed on a Universal Testing Machine (UTM) at 8 mm/min of crosshead speed. The experimental results showed that the fibre with 0° orientation provided the best tensile properties in comparison with fibre orientations of 90° and 0°/90°. As in FML, the incorporation of aluminium layers in the composite laminate improved the stiffness of the composite; 0°, 0°/90° and 90° in that order. However, the tensile strength of FML was lower than its GFRP composite counterpart except for 90° orientation. Analytical prediction for the stiffness and strength of thin FML using metal volume fraction (MVF) method showed a good correlation to the experimental results with the accuracy of 4% – 32% and 2% - 17%, respectively. In conclusion, the fibre orientation significantly influenced the tensile properties of thin GFRP composite and thin FML. The stiffness increased by 7%, 40% and 70% for GFRP composite at fibre orientations of 0°, 0°/90° and 90°, respectively. At 0° and 0°/90° fibre orientations, the GFRP had better tensile strength than FML but the tensile strength of FML was still higher than aluminium. Meanwhile, analytical MVF method can effectively predict the thin FML stiffness and strength.

1.0 INTRODUCTION

A Fiber Metal Laminate (FML) is a sophisticated hybrid composite material made from a mixture of metal and composite laminate [1-5]. FML combines the specific advantages or characteristics of its constituents (metallic materials and fibre composites), such as the high rigidity and strength of composite layers, as well as the plastic behaviour and durability of aluminium alloy [3, 6-7]. These manufactured FMLs have excellent mechanical properties such as high strength-to-weight ratio, high corrosion, impact, fatigue, flame resistance, lower density, high capacity of energy-absorbing, and ease of manufacture [6, 8-11]. Therefore, these advantages promote the FML to replace traditional materials like metals, alloys, and natural fibre in those applications which are prone to fracture [3, 6].

There are numerous studies in the literature on the effects of fibre orientation on composite mechanical performance. H. W. Wang et al. investigated the effect of fibre orientation on the elastic

modulus of unidirectional E-glass fibre reinforced in epoxy resin [12]. The results denoted that the fibre orientation (0° to 90°) has a significant impact on the composite's elastic modulus. When the fibres were oriented in a 0° direction, the composites had the highest value of elastic modulus. The composites had the lowest elastic modulus when the fibres were oriented in a 60° direction. The elastic modulus of the composite slightly increased when the fibres were oriented at an angle greater than 60° . Sessaiah and Reddy reported that the 0° fibre orientation towards the tensile loading significantly improved the mechanical properties of glass fibre-reinforced epoxy composites in that loading direction [13]. Similarly, B. Jena et al., Khalid et al. and Rassiah et al. studied the ultimate stress, ultimate load and elastic modulus of unidirectional carbon fibre composites with different orientations (0° and 90°) [14-16].

However, there is a lack of literature on the effect of fibre orientation on the performance of the FML sandwich structure, especially with small thicknesses. Kamocka and Mania in 2015 attempted an analytical prediction of stiffness and strength of FML based on the well-known rule of mixture, ROM which was originally applied to the unidirectional lamina and laminate [17]. In several studies, thicker FML was investigated such as 3 mm of FML thickness as in Kumar and Harichandan [5] and 2mm of FML in Kamocka and Mania [17].

In the present paper, vacuum bagging and oven curing techniques are used to fabricate thin E-glass fibre prepreg reinforced polymer composite ($t_{GFRP} \leq 0.9$ mm) and thin FML $t_{FML} \leq 1.5$ mm with different fibre orientations (0°), (90°), and ($0^\circ/90^\circ$). Then the thin glass fibre reinforced plastic composite, GFRP and thin FML are subjected to a tensile test as per the ASTM standard. Adapted ROM is used to predict the stiffness and strength of the FML, and the predicted results are compared to the test results. This study aims to investigate the efficiency of ROM prediction for thin FML and the influence of the fibre orientations and stacking sequence on the tensile behaviour of thin GFRP composites and thin FML. Through experimental and analytical works in this paper, it was found that the analytical prediction could predict both tensile elastic modulus and strength for thin FML with a certain degree of accuracy.

2.0 MATERIALS AND METHODS

The metallic material and reinforcement used in this study were aluminium alloy 2024-T3 sheet and Unidirectional (UD) E-glass fibre prepreg respectively to fabricate the GFRP composite and FML laminates. The UD E-glass fibre prepreg was already impregnated with epoxy resin. Table 1 indicates the specifications of the used materials in this research.

Table 1. Specification of materials

Material	Descriptions
Aluminium alloy sheet 2024-T3	Thickness: 0.30 mm
E-glass fibre prepreg	Thickness: 0.04 mm (uncured) Texture: Unidirectional (UD) Areal weight: 170 g/m ²

2.1 Fabrication Process

Using vacuum bagging and oven curing techniques, several laminates of GFRP composites and FML panels with three different fibre orientations, such as 0° , 90° and cross-ply ($0^\circ/90^\circ$) were fabricated. The UD E-glass fibre prepreps and aluminium alloys were cut with a dimension of 350 mm x 320 mm. Eight layers of UD E-glass fibre prepreps were used to fabricate the GFRP composite laminate. To fabricate FMLs, the GFRP composite laminate was stacked between two aluminium alloy layers in a sandwich structure. A pre-treatment process of aluminium alloy surfaces was required before using them in the laminate to increase the adhesive bonding between the GFRP composite laminate and aluminium alloy layers. Initially, the aluminium alloy surfaces were mechanically abraded using an orbital sander with aluminium oxide sandpaper of grit 40 to create a macro-level roughened surface and to remove the oxide layer from the aluminium sheet. Then, the aluminium alloy surfaces were subjected to a series of degreasing steps to produce a free-contamination metal surface. The water-break test was executed to evaluate the hydrophilic state of the abraded aluminium alloy surface. The aluminium alloys and UD E-glass fibre prepreps were stacked based on the desired stacking sequence and layup configuration. The air gaps between the lamina were squeezed out manually using a roller during the laying-up process. Then the laminates were debugged with full pressure at room temperature (RT) to remove the air gaps or voids in

the laminates. Subsequently, the laminates were cured in an oven at 15°C for 30 minutes with 3°C/min of heating and cooling rates. Figure 1 shows the fabricated plate of GFRP composite and FML.

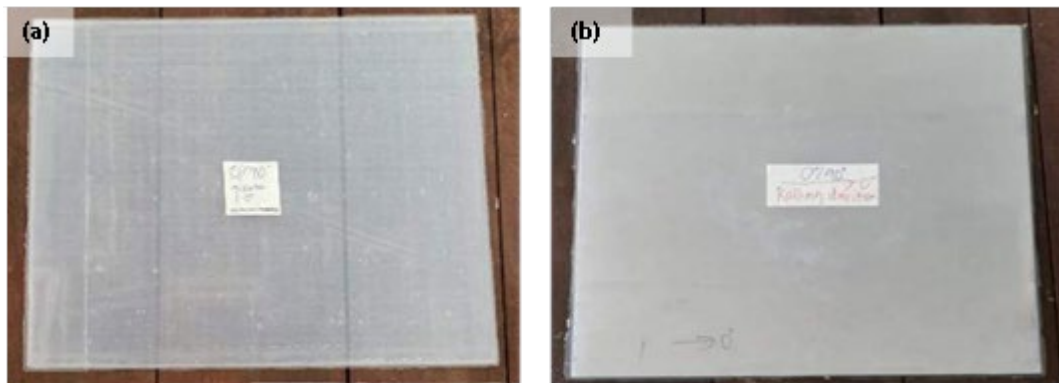


Figure 1. Laminated plate (a) GFRP composite laminate; (b) FML

2.2 Specimen Preparation

The fabricated GFRP composite laminates and FML panels were mechanically cut to the desired dimension (rectangular plate) based on the ASTM D3039 standard as shown in Table 2. The thickness of aluminium alloy, GFRP composite specimens and FML specimens were 0.30 mm, 0.83 mm ~ 0.85 mm and 1.39 mm ~ 1.50 mm respectively. The aluminium alloy sheets were directly cut to the preferred size according to the standard using a foot shearing machine. The GFRP composite laminates and FML panels were cut using a Dremel rotary hand tool and a vertical bend saw machine respectively. Figure 2 shows all the specimens that are cut into the specimen size.

Table 2. Specimen dimension based on the ASTM D3039 standard

Fiber orientation	Dimension, mm
0° - Unidirectional	250 x 15 x t
90° - Unidirectional	175 x 25 x t
0°/90° - Cross ply	250 x 25 x t
Aluminium alloy 2024-T3	250 x 25 x t



Figure 2. Specimens of aluminium alloy 2024-T3, GFRP composite and FML

2.3 Tensile Test

To investigate the influence of three different fibre orientations on the tensile properties of thin GFRP composite, thin FML, and thin monolithic aluminium alloy, the tensile tests were performed at a constant crosshead speed of 8 mm/min on a Universal Testing Machine (UTM) with a maximum load capacity of 50 kN. Three specimens from each orientation of those hybrid materials were tested, including aluminium alloy, and the average tensile properties were determined. Emery clothes were used for composite specimens to prevent gripping damage. Tensile properties of the FML and its constituents, such as elastic modulus and tensile strength were measured during the experiment. Figure 3a shows the UTM and Figure 3b shows the specimen mounted and gripped, ready to be tested.

3.0 ANALYTICAL PREDICTION OF STIFFNESS AND STRENGTH FOR FIBER METAL LAMINATE

The rule of mixture (ROM), as shown in equations 1 and 2 was used to determine the effective longitudinal elastic modulus and longitudinal strength of a lamina from the mechanical properties of its constituents [14]. $E_{1,GFRP}$ is the longitudinal elastic modulus of the composite, E_f and E_m are the elastic modulus of fibre and matrix respectively. Meanwhile, V_f and V_m are volume fractions of fibre and matrix. In equation 2, σ_{max} is the strength of the material with the additional subscripts is used analogously to their use in equation 1. For transverse elastic modulus, the same parameters as in tensile elastic modulus determined its values as shown in equation 3 where $E_{2,GFRP}$ is the transverse elastic modulus of the composite.

$$E_{1,GFRP} = V_f E_f + V_m E_m \quad (1)$$

$$\sigma_{1,GFRP,max} = V_f \sigma_{f,max} + V_m \sigma_{m,max} \quad (2)$$

$$E_{2,GFRP} = \frac{E_f E_m}{V_f E_m + V_m E_f} \quad (3)$$

ROM was further applied to determine the stiffness and strength of fibre metal laminate in the sense of volume fraction of composite laminate and aluminium alloy sheet as demonstrated by Kamocka and Mania in 2015 [17]. Analytical prediction using ROM for FML is shown in equations 4 to 6 where MVF in equation 4 is metal volume fraction according to the metal volume fraction (MVF) method [18-19] and E_{Al} is the elastic modulus of the metal sheet. The MVF is defined by m number of metal sheets in the FML, t_{Al} thickness of the individual metal sheet and t total thickness of the FML.

$$E_{1,FML} = MVF \cdot E_{Al} + (1 - MVF) E_{GFRP} \quad (4)$$

$$\sigma_{1,FML,max} = MVF \cdot \sigma_{Al,max} + (1 - MVF) \sigma_{1,GFRP,max} \quad (5)$$

$$MVF = \frac{m \cdot t_{Al}}{t} \quad (6)$$

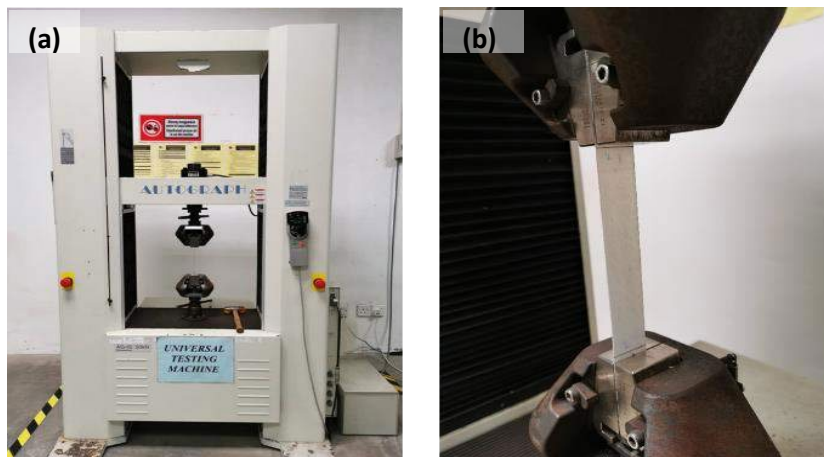


Figure 3. (a) Universal Testing Machine (UTM); (b) Tensile test in UTM

4.0 RESULTS AND DISCUSSION

Figure 4a shows the tensile engineering stress-strain curves of aluminium alloy 2024-T3 (Al 2024-T3). Meanwhile, Figure 4b and Figure 4c show the tensile engineering stress-strain curves of GFRP composites and FMLs with three different fibre orientations respectively. In general, Al 2024-T3 started with elastic deformation followed by large plastic deformation after reaching its yield point. It continued to deform plastically until it reached its breaking point. On the other hand, the curves in Figure 4b clearly show that the GFRP composites were elastically deformed and fractured without significant plastic deformation. There was relatively no plastic deformation that occurs as the GFRP composite with epoxy matrix materials is brittle. Aside from GFRP 90° orientation, GFRP composites could sustain a very high-stress level even though the stress level had already surpassed the ultimate tensile stress of Al 2024-T3, $\sigma_{Al,max}$. The deformation of these GFRPs was elastic only, with no irreversible plastic deformation. However, the aluminium alloy was superior in terms of its ability to sustain high strains before failure compared to GFRP due to its ductility and ability to deform with such a high plastic strain. Thus, it was expected that the ductility of the alloy and the brittleness of the GFRP would significantly determine the behaviour and failure of FML under tensile loading. Originally, the GFRP composite has a linear response and high strength value, but it was observed that some curvature presents in the stress-strain curve of its FML counterpart as can be seen in Figure 4c. In FML, once the yield stress of Al 2024-T3 was reached, the alloy would continue to deform plastically, and meanwhile its GFRP constituents would continue its deformation elastically. Effectively, these two constituents experienced the same magnitude of deformation but with different types of strains. The plastic strains of the Al 2024-T3 layer gave some nonlinearity to the FML stress-strain curve, notably starting at a stress value around 149 MPa which was the yield point of Al 2024-T3. The nonlinearity was more obvious for FML 0°/90° and FML 90° as the GFRP constituents of these specimens possessed significantly lower elastic modulus compared to GFRP 0°. Thus FML 0°/90° and FML 90° were more affected by the ductility of the Al 2024-T3 compared to FML 0° which can be observed in Fig 5a to Figure 5c. The elastic modulus of FML 0°/90° in Figure 5b and FML 90° in Figure 5c increased by 39.80% and 69.51%, respectively. However, the FML 0° still possessed the highest elastic modulus compared to FML 0°/90° and FML 90° with an increment of 7.32%.

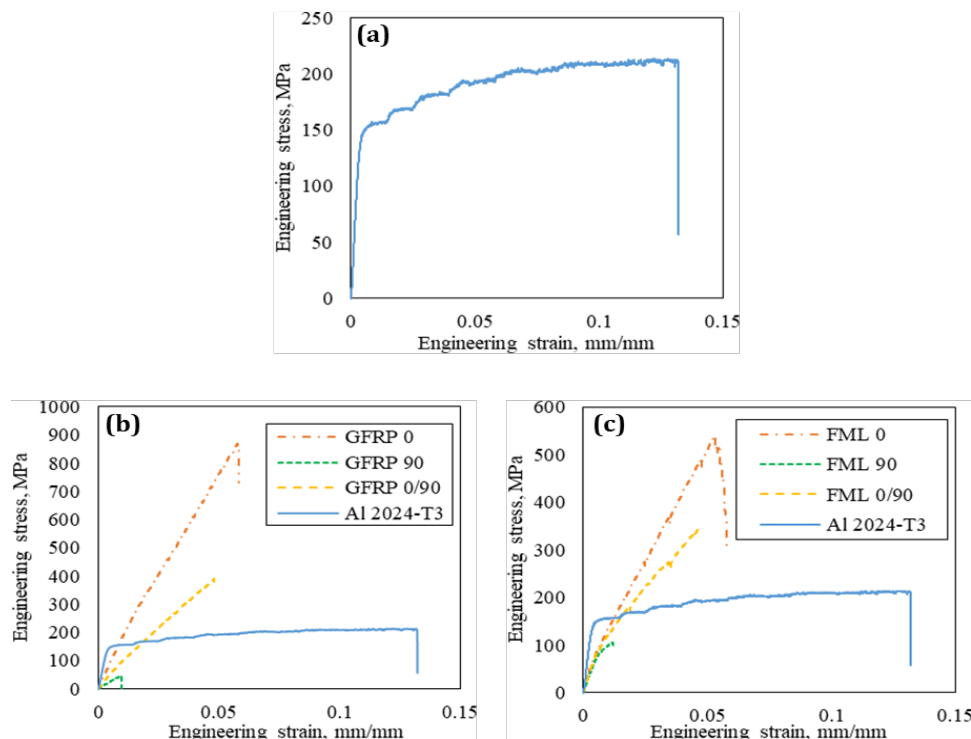


Figure 4. Representative curves of engineering stress vs engineering strain of (a) Al 2024-T3; (b) GFRP composites (0°, 90° and 0°/90°); (c) FMLs (0°, 90° and 0°/90°)

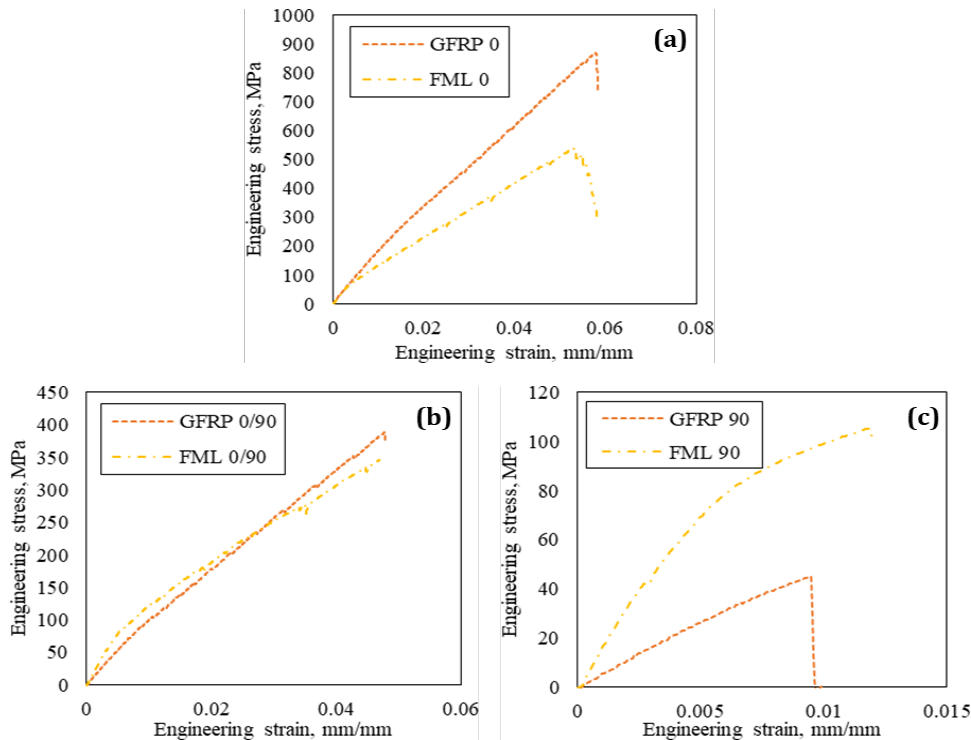


Figure 5. Representative curves of engineering stress vs engineering strain of GFRP composite and FMLs at (a) 0°; (b) 0°/90°; (c) 90° fiber orientations

4.1 Tensile Stiffness Of GFRP And FML

From the results obtained, the GFRP composite specimens exhibited the highest elastic modulus when the fibre orientation was set at 0° (18.48 GPa), followed by cross-ply 0°/90° (10.80 GPa) and 90° (5.44 GPa) as shown in Figure 6. In the case of 0° fibre orientation of a GFRP composite specimen, all the fibres were in the same direction and parallel to the loading direction. According to the rule of mixtures (ROM) analysis, the fibre properties would be dominant in the loading direction wherein the fibre stress would be higher than the matrix stress at a specific elastic strain. Furthermore, the fibre had a larger tensile modulus than the matrix [20] which results in GFRP with 0° fibre orientation exhibiting the highest elastic modulus. When the tensile load was applied, the load was evenly spread across all the fibres and transferred along the fibre direction. Then, all fibres would carry most of the load. The elastic modulus of the composite would be affected when changing the volume fraction of fibre in the composite as expressed in equation 1. In the case of 90° fibre orientation, the tensile load was applied perpendicular to the fibre direction which caused the dominance of fibre properties to fade and matrix properties to take over. When the fibres were aligned at cross-ply (0°/90°), the direction of the fibres was not all parallel to the loading direction. The tensile load pulled the fibre in the direction of 0° providing high stiffness, but the fibre in the direction of 90° did not effectively provide the stiffness in the direction of the load. Based on this ROM analysis, it was logical that the experiment results indicate that ($E_{1,GFRP,0} > E_{1,GFRP,0/90} > E_{1,GFRP,90}$).

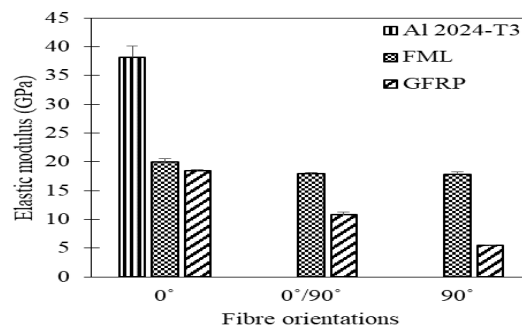


Figure 6. Elastic modulus of GFRP composite and FML at 0°, 90° and 0°/90° fibre orientations and aluminium alloy 2024-T3 (n=3)

The elastic modulus obtained by FML at 0°, 90° and 0°/90° fibre orientations were 19.94 GPa, 17.84 GPa and 17.94 GPa, respectively. Meanwhile, the elastic modulus of Al 2024-T3 was $E_{Al} = 38.18$ GPa. Figure 6 shows that the FML with 0° fibre orientation provided the highest elastic modulus and the FML with 90° fibre orientation had the least elastic modulus. In summary, $(E_{1,FML,0} > E_{1,FML,0/90} > E_{1,FML,90})$ with its pattern was similar to the GFRP. This pattern was analytically explained by the MVF method as in equation 4. The second term in the MVF relationship indicates that the elastic modulus of FML is heavily dependent on the elastic modulus of its GFRP constituent. Table 3 tabulates the comparison of elastic modulus obtained from the experiment and the MVF analytical prediction. Analytically, the value and pattern of elastic modulus for FML with various orientations correlated well with the experimental results. The MVF method predicted the FML 90° very well with a small error of 3.9%. Meanwhile, it over-predicted the elastic modulus of FML 0° with a 32.2% error.

In addition to the pattern, the elastic modulus of FML was obviously larger than its GFRP composite, as shown in Figure 5 to 6. Clearly that adding the Al 2024-T3 layer to GFRP increased its tensile stiffness. However, the rate of increment for the elastic modulus of GFRP to its FML counterpart varied between fibre orientations. For GFRP 0°, its elastic modulus was 18.48 GPa which then only improved to 19.94 GPa of its FML counterpart, i.e., an 8% increment. Meanwhile, the increment in FML 90° and 0°/90° were relatively higher than FML 0° with 228% and 66% respectively. Thus, the improvement in terms of elastic modulus was very little and almost insignificant for FML 0°, but very significant for FML 90° and FML 0°/90°.

In summary, both GFRP and FML with fibre orientation of 0° had the highest elastic modulus followed by 0°/90° and 90°. The elastic modulus of FML was influenced by the low elastic modulus of GFRP and the relatively superior elastic modulus and plasticity of aluminium alloy [19, 21-22]. These experimental results were also supported analytically by ROM analysis and the MVF method. Mechanically, aluminium alloy requires greater stress compared to GFRP composites to deform within the elastic range for an amount of elastic strain which as a result would cause an increment of elastic modulus in FML from its GFRP counterpart. Overall, the elastic modulus of the aluminium alloy specimen (38.18 GPa) was higher than that of FML and GFRP composite $(E_{1,Al} > E_{1,FML} > E_{1,GFRP})$ with respect to the orientations. These results were also supported by experimental results that were published in other literature [23-24]. Conclusively, aluminium alloy enhanced the elastic modulus of the GFRP the way the fibre enhanced the elastic modulus of overall GFRP as explained by ROM analysis [25].

4.2 Tensile Strength Of GFRP And FML

Figure 7 shows the tensile strength of both the GFRP composite and FML. The tensile strength of the GFRP composite with 0°, 90°, and 0°/90° fibre orientations were 851.56 MPa, 45.83 MPa and 406.57 MPa respectively. In the order of $(\sigma_{1,GFRP,0,max} > \sigma_{1,GFRP,0/90,max} > \sigma_{1,GFRP,90,max})$, it had the same pattern as the elastic modulus of the GFRP composite which can be observed in Figure 6 and Figure 7. The tensile strength displayed a high value when the fibre orientation was 0° because the continuous fibres provide the load-bearing capacity. The strength of GFRP 90° was significantly lower as the load-bearing capacity was only provided by the matrix's strength and the bonding strength between the matrix and fibres [26–31]. Meanwhile, FMLs had the tensile strength of 521.35 MPa, 97.27 MPa, and 338.02 MPa respectively, with fibre orientations of 0°, 90°, and 0°/90°. Similar to elastic modulus, the strength of FML was heavily dependent on the strength of its constituents, thus followed the pattern of $(\sigma_{1,FML,0,max} > \sigma_{1,FML,0/90,max} > \sigma_{1,FML,90,max})$. This pattern was also logical as described by the analytical MVF method for strength in equation 5 where it indicates that the strength of FML is heavily dependent on the strength of its GFRP constituent.

As shown in Figure 7, the tensile strength of FML was lower than that of the GFRP composite but higher than that of aluminium alloy $(\sigma_{1,GFRP,max} > \sigma_{1,FML,max} > \sigma_{1,Al,max})$ except for FML 90°. FML 90° had almost a double tensile strength than its GFRP. This was simply because the strength of GFRP at 90° was mainly sourced from the strength of the matrix. Thus, the strength of FML 90° was significantly enhanced by the strength of aluminium. Figure 7 showed that the strength of GFRP 0° and GFRP 0°/90° was away above Al. When the GFRP 0° and GFRP 0°/90° combined with Al, the strength of FML 0° and FML 0°/90° was in the middle which is apparently lower than GFRP 0° and GFRP 0°/90°, respectively. However, the strength of GFRP 90° was away below Al. When the GFRP 90° combined with Al, the strength of FML 90° was still in the middle and higher than GFRP 90° but below Al. In this study, the MVF was around 0.4. From the analytical prediction using the MVF method as tabulated in Table 3, the error compared to

experimental results ranges from 2.3% to 16.9% which was generally more accurate than the elastic modulus analytical prediction. Other than FML 90°, the strength of FML for each orientation was almost the average between the strength of Al 2024-T3 and the strength of its GFRP constituents. The pattern of this result was also supported by finite element analysis and experimental results that were obtained from P. Soltani et al., G. Wu and J.-M. Yang, P. Mathivanan et al., and S. Ebrahim Moussavi-Torshizi et al. [23], [24], [32], [33].

Relatively, the aluminium alloy would subsequently undergo plastic deformation before failing, meanwhile GFRP composite would still undergo elastic deformation under the same total strain as can be observed in Figure 4b. Effectively in the FML specimen, under the load that caused the aluminium alloy to experience stress higher than its yield stress, the aluminium alloy layers had started to deform plastically meanwhile the GFRP layers would continue to deform elastically. The combination of deformation types can be observed by the little curvature of the stress-strain curve of FML in Figure 4c to 5. This condition was sustained until the stress within the GFRP composite had surpassed its ultimate tensile strength, $\sigma_{1,GFRP,max}$. At this stage, the Al 2024-T3 layer was still undergoing plastic deformation, and the strain experienced was still far away from the failure strain. Subsequently, the FML failed due to the failure and breakage of its GFRP constituents. Figure 8 shows the elongated and buckled Al 2024-T3 layer after failure. As discussed earlier, the Al 2024-T3 layer deformed permanently before failure but not for the GFRP composite. When the tensile machine grip was removed after the FML specimen had failed, the remaining composite layers which only deformed elastically and were not broken retracted back the whole FML to its original length. On the other hand, the Al 2024-T3 layer which had permanently lengthened was also forced to retract to the FML original length. As a result, the alloy layer delaminated from GFRP, especially at the mid-section of the FML and then buckled to compensate the FML that has retracted to its original length.

In summary, the high tensile strength of the GFRP composite enhanced the strength of FML, whereas the aluminium alloy that was superior in terms of stiffness enhanced the stiffness of FML. The obtained results were similar to those reported by P. Soltani et al., S. Ebrahim Moussavi-Torshizi et al., and E. C. Botelho et al. [23], [33], [34]. Overall, the thin FML with a fibre orientation of 0° exhibited higher tensile properties (tensile strength and tensile modulus) than the thin FML with an off-axis angle (90°) and cross-ply (0°/90°) as shown in Figure 6 and Figure 7. These findings were effectively predicted by rule of mixture (ROM) and metal volume fraction (MVF) method with a certain degree of accuracy. Comparatively, the analytical prediction for thin FML's tensile strength was more accurate than the analytical prediction for thin FML's tensile elastic modulus. In all thin FML specimens, when the load exceeds the yield stress of the aluminium alloy, the load was further carried with both elastic strains occurring in GFRP composite and plastic strain in aluminium alloy. Subsequently, the composite constituent in the FML would reach its maximum strain and fail which caused the composite to break and the thin FML to fail.

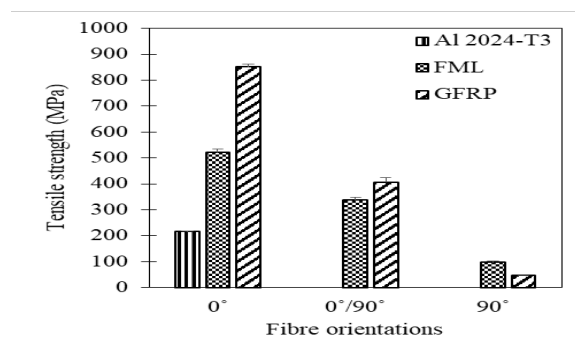


Figure 7. Tensile strength of GFRP composite and FML at 0°, 90° and 0°/90° fibre orientations and aluminium alloy 2024-T3 (n=3)

Table 3. Experimental and analytical results of stiffness and strength of FML

Mechanical Properties	Experiment results (n=3)	Analytical prediction	Error (%)
Longitudinal elastic modulus of FML [Al/0 ₄] _s $E_{1,FML,0}$ (GPa)	19.94±0.62	26.36	32.20
Longitudinal elastic modulus of FML	17.84±0.39	18.54	3.90

Mechanical Properties	Experiment results (n=3)	Analytical prediction	Error (%)
[Al/90 ₄] _s $E_{1,FML,90}$ (GPa)			
Longitudinal elastic modulus of FML	17.94±0.23	21.75	21.25
[Al/0 ₂ /90 ₂] _s $E_{1,FML,0/90}$ (GPa)			
Longitudinal strength of FML [Al/0 ₄] _s	521.35±12.50	597.18	14.54
$\sigma_{1,FML,0,max}$ (MPa)			
Longitudinal strength of FML [Al/90 ₄] _s	97.27±4.73	113.74	16.93
$\sigma_{1,FML,90,max}$ (MPa)			
Longitudinal strength of FML [Al/0 ₂ /90 ₂] _s	338.02±10.31	330.19	2.32
$\sigma_{1,FML,0/90,max}$ (MPa)			



Figure 8. Plastic deformation and delamination of Al 2024-T3 layer post failure

5.0 CONCLUSION

In this research study, GFRP composites and thin FMLs were developed using vacuum bagging and oven curing technique with different fibre orientations [0°]₈, [90°]₈, [(0°)₂/(90°)₂]_s, [Al/(0°)₄]_s, [Al/(90°)₄]_s, and [Al/(0°)₂/(90°)₂]_s. These materials were subjected to a tensile test to examine the tensile elastic modulus and the tensile strength. Further, the experimental results were compared to the analytical prediction using the ROM/MVF method. It can be concluded that the thin FML with a fibre orientation of 0° exhibits the highest tensile properties (tensile strength and tensile elastic modulus) than the FML with an off-axis angle (90°) and cross-ply (0°/90°). The order of the tensile elastic modulus and strength are respectively; ($E_{1,FML,0} > E_{1,FML,0/90} > E_{1,FML,90}$) and ($\sigma_{1,FML,0,max} > \sigma_{1,FML,0/90,max} > \sigma_{1,FML,90,max}$). In all thin FML specimens, when the load exceeds the yield stress of the aluminium alloy, the load is further carried with both elastic strains occurring in GFRP composite and plastic strain in aluminium alloy. Subsequently, composite constituents in the FML will reach their maximum strain which causes the composite to break and FML to fail. As for an analytical prediction, the metal volume fraction (MVF) method which is adapted from the rule of mixture (ROM) is proven can predict the tensile elastic modulus and strength of thin fibre metal laminate (FML). Accuracy for elastic modulus prediction was in the range of 4% – 32% and for strength was in the range of 2% - 17%. Conclusively, analytical prediction using MVF for strength is more accurate than for elastic modulus. The MVF method can also effectively explain the correlation between the tensile properties of the thin FML to its corresponding GFRP composite and aluminium alloy constituents.

In this paper, the study was limited to symmetry unidirectional and cross-ply orientation FML. Thus, this study can be further extended to thin FML with other orientations and stacking configurations. The finding in this paper should allow a better understanding on how tensile properties of aluminium alloy 2024-T3 and GFRP enhanced the elastic modulus and strength in their FML form. All the discussions and findings could be the basis in explaining the behaviour and failure of FML in other types and complexity of loading such as compressions, dynamic, impact and even explosion. These findings would be advantageous in designing and manufacturing of thin structures in various industries that are already using or have the potential to apply FML as their main materials.

6.0 ACKNOWLEDGEMENT

Great appreciation to the School of Engineering (Aerocomposite Laboratory), Universiti Sains Malaysia (USM) and Strength Laboratory, Universiti Teknologi MARA (UiTM) for supporting the fabrication

activities and experimental works respectively. This project is funded by the Ministry of Higher Education (MOHE) of Malaysia, ref no. FRGS/1/2018/TK03/UiTM/02/5. Thank you to Universiti Teknologi MARA, Malaysia for various and generous assistance throughout the project until completion.

List of Reference

- [1] Hariharan, E., & Santhanakrishnan, R. (2016). Experimental analysis of fiber metal laminate with aluminium alloy for aircraft structures. *Int. J. Eng. Sci. Res. Technol*, 9655(5), 94-102.
- [2] Salve, A., Kulkarni, R., & Mache, A. (2016). A review: fiber metal laminates (FML's)-manufacturing, test methods and numerical modeling. *International Journal of Engineering Technology and Sciences*, 3(2), 71-84.
- [3] Kashfi, M., Majzoobi, G. H., Bonora, N., Iannitti, G., Ruggiero, A., & Khademi, E. (2017). A study on fiber metal laminates by using a new damage model for composite layer. *International Journal of Mechanical Sciences*, 131, 75-80.
- [4] Vasumathi, M., & Murali, V. (2013). Effect of alternate metals for use in natural fibre reinforced fibre metal laminates under bending, impact and axial loadings. *Procedia engineering*, 64, 562-570.
- [5] Harichandan, A., & Kumar, K. V. (2016). Study on tensile behaviour of carbon jute aluminium-fibre metal laminates. *International journal of mechanical and production engineering*, 2320-2092.
- [6] Sathyaseelan, P., Logesh, K., Venkatasudhahar, M., & Dilip Raja, N. (2015). Experimental and Finite Element Analysis of Fibre Metal Laminates (FML'S) subjected to tensile, flexural and impact loadings with different stacking sequence. *International Journal of mechanical & mechatronics Engineering*, 15(3), 23-27.
- [7] Sinke, J. (2009). Manufacturing principles of fiber metal laminates. In *ICCM-17: International Conference on Composite Materials 2009* (pp. 1-10). IOM.
- [8] Bidgoli, A. M. M., & Heidari-Rarani, M. (2016). Axial buckling response of fiber metal laminate circular cylindrical shells. *Structural Engineering and Mechanics*, 57(1), 45-63.
- [9] Hombergmeier, E. (2006, September). Development of advanced laminates for aircraft structures. In *Proceedings of 25th International Congress of the Aeronautical Sciences* (pp. 3-8).
- [10] Ekşi, S., & Genel, K. (2017). Comparison of mechanical properties of unidirectional and woven carbon, glass and aramid fiber reinforced epoxy composites. *Acta Physica Polonica A*, 132(3), 879-882.
- [11] Zhen, C. (2015). Review on the dynamic impact characteristics of fiber metal laminates. *Journal of Advanced Review on Scientific Research*, 16(1), 1-11.
- [12] Wang, H. W., Zhou, H. W., Gui, L. L., Ji, H. W., & Zhang, X. C. (2014). Analysis of effect of fiber orientation on Young's modulus for unidirectional fiber reinforced composites. *Composites part B: engineering*, 56, 733-739.
- [13] Seshaiyah, T., & Reddy, V. K. (2018). Effect of fiber orientation on the mechanical behavior of e-glass fibre reinforced epoxy composite materials. *Int. J. Mech. Prod. Eng. Res. Devel.(IJMPERD)*, 379-396.
- [14] Jena, B., Khan, S. Z., Mohanty, B. B., & Surabhi, S. (2016). Experimental Study on Effect of Fiber Orientation on the Tensile Properties of Fabricated Plate Using Carbon Fiber. *International Journal of Civil Engineering (IJCE)* 5.4: 9, 16.
- [15] Khalid, S. N. A., Zainulabidin, M. H., Arifin, A. M. T., Hassasn, M. F., Ibrahim, M. R., & Rahim, M. Z. (2018). Mechanical performances of twill kenaf woven fiber reinforced polyester composites. *International Journal of Integrated Engineering*, 10(4).
- [16] Rassiah, K., Ali, A., & Saeman, M. (2021). Evaluation the Effect of Laminated Layer Sequence of Plain-Woven Bamboo on Tensile and Impact Performance of E-glass Woven/Epoxy Hybrid Composites. *International Journal of Integrated Engineering*, 13(7), 194-200.
- [17] Kamocka, M., & Mania, R. J. (2015). Analytical and experimental determination of fml stiffness and strength properties. *Mechanics and Mechanical Engineering*, 19(2), 141-159.
- [18] Ergun, H., Liaw, B. M., & Delale, F. (2018). Experimental-theoretical predictions of stress-strain curves of glare fiber metal laminates. *Journal of Composite Materials*, 52(1), 109-121.
- [19] Wu, G., & Yang, J. M. (2005). The mechanical behavior of GLARE laminates for aircraft structures. *Jom*, 57, 72-79.
- [20] Meyers, M. A., Chen, P. Y., Lin, A. Y. M., & Seki, Y. (2008). Biological materials: Structure and mechanical properties. *Progress in materials science*, 53(1), 1-206.
- [21] Bieniaś, J., Jakubczak, P., & Surowska, B. (2017). Properties and characterization of fiber metal laminates. In *Hybrid polymer composite materials* (pp. 253-277). Woodhead Publishing.

- [22] Kawai, M., Morishita, M., Tomura, S., & Takumida, K. (1998). Inelastic behavior and strength of fiber-metal hybrid composite: Glare. *International Journal of Mechanical Sciences*, 40(2-3), 183-198.
- [23] Soltani, P., Keikhosravi, M., Oskouei, R. H., & Soutis, C. (2011). Studying the tensile behaviour of GLARE laminates: a finite element modelling approach. *Applied Composite Materials*, 18, 271-282.
- [24] Wu, G., & Yang, J. M. (2005). Analytical modelling and numerical simulation of the nonlinear deformation of hybrid fibre-metal laminates. *Modelling and Simulation in Materials Science and Engineering*, 13(3), 413.
- [25] Carrillo, J. G., Gonzalez-Canche, N. G., Flores-Johnson, E. A., & Cortes, P. (2019). Low velocity impact response of fibre metal laminates based on aramid fibre reinforced polypropylene. *Composite Structures*, 220, 708-716.
- [26] Abramovich, H. (2017). Introduction to composite materials. In *Stability and vibrations of thin walled composite structures* (pp. 1-47). Woodhead Publishing.
- [27] Mohd Nurazzi, N., Khalina, A., Chandrasekar, M., Aisyah, H. A., Ayu Rafiqah, S., Ilyas, R. A., & Hanafee, Z. M. (2020). Effect of fiber orientation and fiber loading on the mechanical and thermal properties of sugar palm yarn fiber reinforced unsaturated polyester resin composites. *Polimery*, 65.
- [28] Cordin, M., Bechtold, T., & Pham, T. (2018). Effect of fibre orientation on the mechanical properties of polypropylene-lyocell composites. *Cellulose*, 25, 7197-7210.
- [29] Vasudevan, A., Pandiyarajan, R., Kumar, B. N., & Vijayarangam, J. (2020, December). Effect of Kevlar ply orientation on mechanical characterization of Kevlar-glass fiber laminated composites. In *IOP Conference Series: Materials Science and Engineering* (Vol. 988, No. 1, p. 012088). IOP Publishing.
- [30] Groves, S. E. (1986). A study of damage mechanics in continuous fiber composite laminates with matrix cracking and internal delaminations. Texas A&M University.
- [31] Parmiggiani, A., Prato, M., & Pizzorni, M. (2021). Effect of the fiber orientation on the tensile and flexural behavior of continuous carbon fiber composites made via fused filament fabrication. *The International Journal of Advanced Manufacturing Technology*, 114, 2085-2101.
- [32] Mathivanan, P., Balakrishnan, M., & Krishnan, H. (2010). Metal thickness, fiber volume fraction effect on the tensile properties, debonding of hybrid laminates. *Journal of reinforced plastics and composites*, 29(14), 2128-2140.
- [33] Moussavi-Torshizi, S. E., Dariushi, S., Sadighi, M., & Safarpour, P. (2010). A study on tensile properties of a novel fiber/metal laminates. *Materials Science and Engineering: A*, 527(18-19), 4920-4925.
- [34] Botelho, E. C., Silva, R. A., Pardini, L. C., & Rezende, M. C. (2006). A review on the development and properties of continuous fiber/epoxy/aluminum hybrid composites for aircraft structures. *Materials Research*, 9, 247-256.